Effects of layered structural features on charge/orbital ordering in $(La, Sr)_{n+1}Mn_nO_{3n+1}$ (n = 1 and 2)

2009 J. Phys.: Condens. Matter 21 045601

(http://iopscience.iop.org/0953-8984/21/4/045601)

J. Phys.: Condens. Matter **21** (2009) 045601 (6pp) doi:10.1088/0953-8984/21/4/045601

Effects of layered structural features on charge/orbital ordering in $(La, Sr)_{n+1}Mn_nO_{3n+1}$ ($n = 1$ and 2)

C Ma, H X Yang, L J Zeng, Z A Li, Y Zhang, Y B Qin and J Q Li[1]

Beijing National Laboratory for Condensed Matter Physics, Institute of Physics, Chinese Academy of Sciences, Beijing 100080, People's Republic of China

E-mail: Ljq@aphy.iphy.ac.cn

Received 15 July 2008, in final form 13 November 2008
Published 22 December 2008
Online at stacks.iop.org/JPhysCM/21/045601

Abstract

The charge/orbital ordering (COO) of the layered mixed-valence manganites $(La, Sr)_{n+1}Mn_nO_{3n+1}$ ($n = 1$ and 2) is examined by first-principles calculations and discussed in comparison with the $La_{0.5}Ca_{0.5}MnO_3$ perovskite phase ($n = \infty$). The results demonstrated that the layered structural features could yield not only visibly weak coupling between Mn–O layers but also various features in the orbital ordering associated with different types of local structural distortions. In both $La_{0.5}Sr_{1.5}MnO_4$ ($n = 1$) and $LaSr_2Mn_2O_7$ ($n = 2$) phases, the orbital ordering can be chiefly assigned to the $d_{x^2-y^2}$ orbital, in contrast with the zigzag-type d_{z^2} orbital ordering in the $n = \infty$ perovskite phase. Our theoretical analysis shows that a variety of essential factors, including the local structural distortions of the MnO_6 octahedra, the on-site Coulomb interaction, and magnetic interaction, have to be properly considered in order to achieve acceptable COO ground states for the layered variants in $(La, Sr)_{n+1}Mn_nO_{3n+1}$.

(Some figures in this article are in colour only in the electronic version)

Layered mixed-valence manganese oxides with the general composition $(R, A)_{n+1}Mn_nO_{3n+1}$ (where R and A are rare- and alkaline-earth ions respectively) have attracted considerable interest because of their peculiar physical properties and phenomena, such as colossal magnetoresistance (CMR) [1], complex phase separations [2, 3], and charge ordered stripes [4, 5]. Moreover, the charge/orbital ordering (COO) accompanied with the metal–insulator transition [6] is another interesting phenomenon extensively investigated in this kind of material in the literature [7]. The orbital ordering [8] plays a key role in the characteristics of exchange interaction and is needed for understanding the magnetic and electric properties. Though the experimental techniques, such as neutron and x-ray scattering, and electron microscopy, have been extensively used to characterize the COO by detecting the induced structural modulations [9–12], it has so far been very difficult to directly observe the COO. A fundamental issue discussed in the recent studies is about the origin of the COO, and various authors have emphasized different mechanisms, such as the on-site Coulomb interaction [13], the Jahn–Teller (JT) coupling [14], and the electrostatic repulsions [15, 16]. Actually, the mechanism and certain critical features of the COO in manganites are still important open questions debated in recent studies [17, 18]. In this work, we perform first-principles calculations for $La_{0.5}Ca_{0.5}MnO_3$, $La_{0.5}Sr_{1.5}MnO_4$, and $LaSr_2Mn_2O_7$, respectively. According to the theoretical results, we analyzed the electronic structural features in different layered phases and discussed the mechanism of the COO in manganites.

The electronic structure calculations were carried out using the full potential linear augmented plane wave (LAPW) method within density functional theory (DFT) via the Wien2k code [19], and we chose the generalized gradient approximation (GGA) as the exchange–correlation potential. The basic layered structures without distortions for these compounds are illustrated in figure 1. The following calculations are based on the distorted structures, and the detailed structural parameters of these three compounds are cited from [20–22]. We also carried out structural optimization in which the entropy is not included, and the obtained results

[1] Author to whom any correspondence should be addressed.

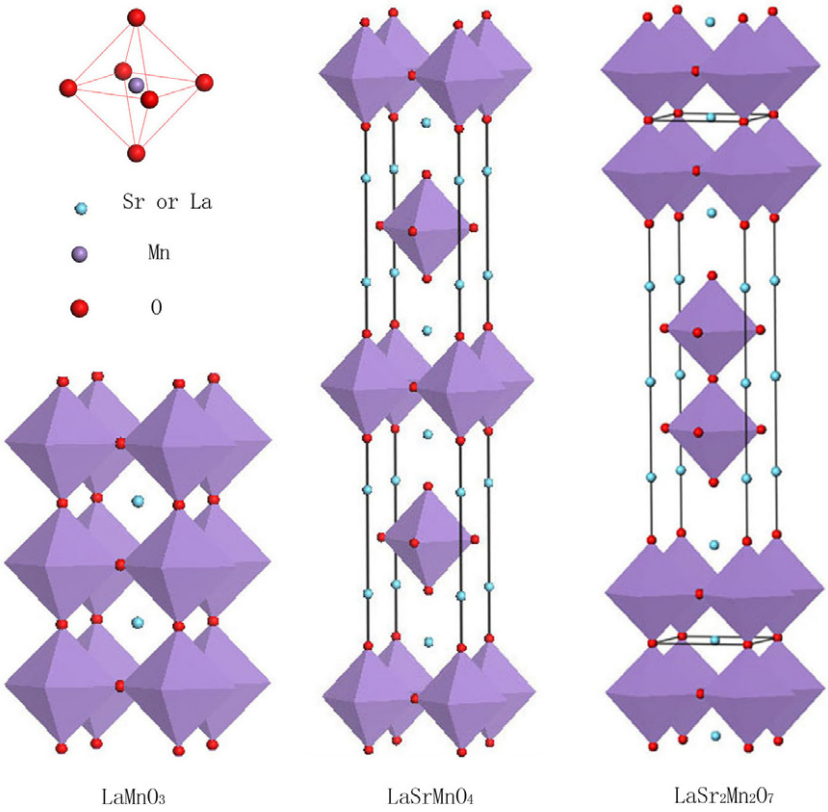

Figure 1. Crystal structures of $(La, Sr)_{n+1}Mn_nO_{3n+1}$ with $n = 1, 2$, and ∞. The MnO_6 octahedron is also shown.

are consistent with the experimental data. The muffin-tin radii R_{mt} were selected as 2.0 au for Mn atoms, 2.1 au for La or Sr atoms, and 1.5 au for O atoms, and $R_{mt}K_{max}$ was set to 7.0 to determine the basis size. The virtual crystal approximation (VCA), which has been proved to be a good method and is extensively used in doped systems, was employed to treat the doping effect. In addition, we also carried out supercell calculations created in consideration of the cation ordering, and the results agree well with that of the VCA.

In order to reveal the fundamental properties of the COO ground states for these mixed-valence manganites, we have performed electronic structure calculations using GGA + U for three layered compounds. Structural distortions and different magnetic structures are also considered for achieving better conclusions comparable to the reported experimental data. The on-site Coulomb interaction is used as $U = 5$ eV [14] for Mn ions to explore the correlation effects in 3d electrons, where we use $U_{eff} = U - J$ and $J = 0$. Both ferromagnetic (FM) and antiferromagnetic (AFM) configurations are considered for the low-temperature charge ordered states. According to experimental findings, the CE-type AFM magnetic structure was used for $La_{0.5}Ca_{0.5}MnO_3$ and $La_{0.5}Sr_{1.5}MnO_4$ [7], and the A-type AFM structure for $LaSr_2Mn_2O_7$ [23]. Based on our systematic theoretical results, we found that provided there are local structural distortions and AFM magnetic structures at low temperatures, the GGA + U method can give rise to the insulating COO ground states for all three phases. Our careful analysis reveals that for the fixed distorted structure, the same COO pattern can be stabilized for both FM and AFM states, suggesting that the obtained COO patterns are not sensitive to spin ordering as discussed in [24].

The average valence state of Mn ions is +3.5 in all three COO phases concerned in the present study, therefore, there would be three 3d electrons in the low-lying t_{2g} orbitals (d_{xy}, d_{xz} and d_{yz}) and the rest in the high-lying e_g orbitals (d_{z^2} and $d_{x^2-y^2}$), based on the Hund's rule and the ligand field effect. In the following context, we will focus our attention on the charge distribution between two distinct Mn sites (so-called Mn^{3+} and Mn^{4+} ions) in the COO ground states. Moreover, the electron density in d_{z^2} and $d_{x^2-y^2}$ orbitals will also be analyzed in correlation with layered structural features. Figure 2 shows the band structures near the Fermi level (E_F) for two COO phases ($n = 1, 2$) in the AFM states as calculated by GGA + U ($U = 5$ eV). It is notable that the presence of energy gaps at E_F directly suggests insulating ground states for both compounds. The dominant electronic states in the gap region are the Mn-e_g orbitals of the majority spin. Due to the coupling between Mn–O layers, these specific layered structures exhibit different bandwidths and dimensionalities which would effectively influence the orbital fluctuation [6, 8].

Careful analysis shows that the orbital occupancies and charge density are visibly different between the nominal $Mn1^{3+}$ and $Mn2^{4+}$ sites, as listed in table 1. Actually, the charge difference is relatively small, especially for $LaSr_2Mn_2O_7$, as shown in the projected density of states (figure 3). The chief differences among the three layered compounds lie in the orbital occupancies of the e_g orbitals, that is they exhibit different orbital ordering patterns. Figure 4

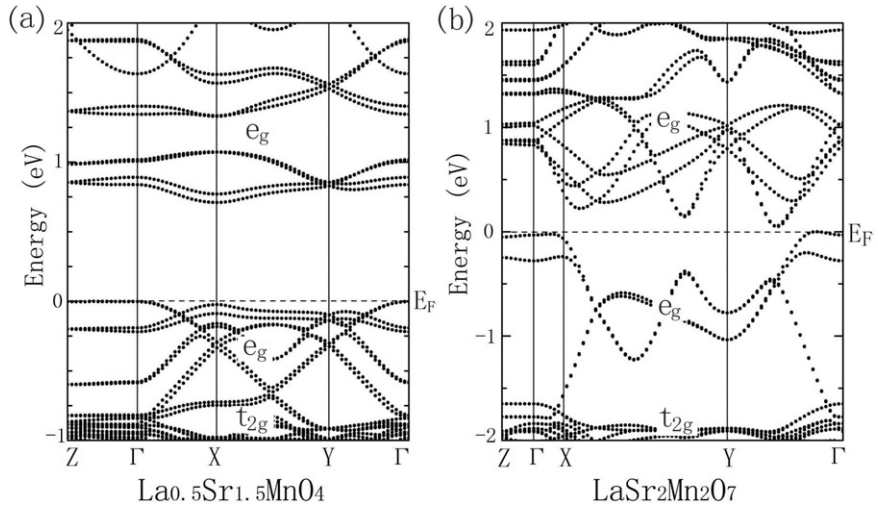

Figure 2. Band structures in the AFM states calculated by the GGA + U method for $La_{0.5}Sr_{1.5}MnO_4$ (a) and $LaSr_2Mn_2O_7$ (b). Γ–X, Γ–Y, and Γ–Z are along the a^*, b^*, and c^* directions in the reciprocal space, respectively. The dashed lines denote the Fermi level at zero energy.

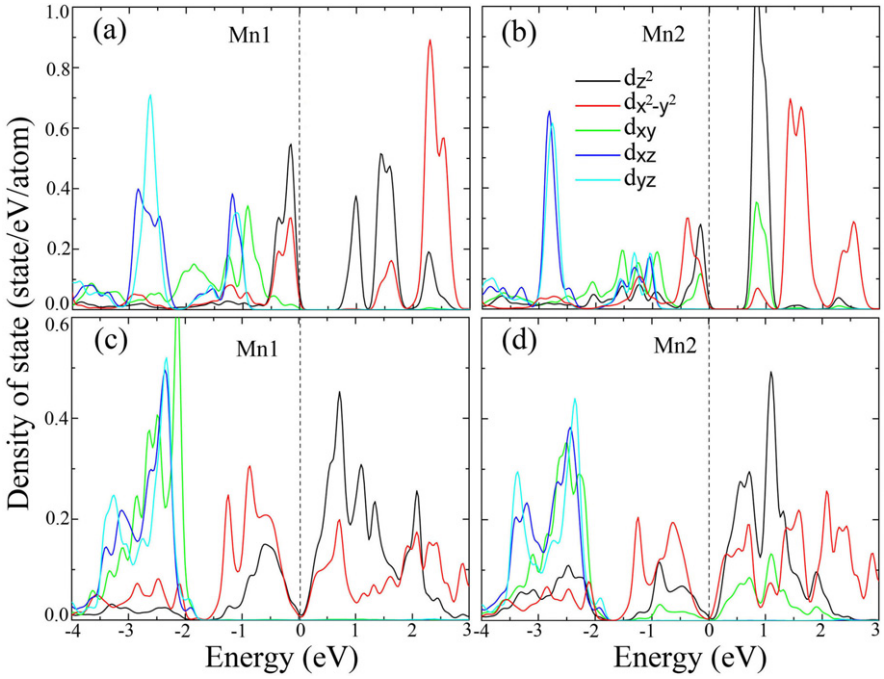

Figure 3. Projected density of states towards 3d orbitals of the nominal Mn^{3+} and Mn^{4+} ions for $La_{0.5}Sr_{1.5}MnO_4$ ((a) and (b)), and $LaSr_2Mn_2O_7$ ((c) and (d)). Only the states of the majority spin are shown. Due to the different local coordinates for different Mn sites, the specific orbital ordering patterns can be seen more clearly in the charge density plot (figure 4). The Fermi energy (E_F) (dashed lines) is set to zero energy.

illustrates the isosurfaces of charge density corresponding to the majority-spin e_g bands below E_F (figure 2(a)) for $La_{0.5}Sr_{1.5}MnO_4$. The local coordinates are selected with the z-axis pointing to the c-axis and the x and y axes pointing to the neighboring O ions in the crystal ab plane, as indicated by the solid arrows in figure 4(a). It is recognizable that both d_{x^2} (d_{y^2}) and $d_{y^2-z^2}$ ($d_{x^2-z^2}$) orbitals are partially occupied and that one orbital outweighs the other one depending on the specific structural distortions of MnO_6 octahedra. Such a phenomenon is considered to result from the orbital occupancy fluctuations within the twofold e_g orbitals [8]. The cooperative Jahn–Teller (JT) distortions commonly existing in transition metal oxides would lift this degeneracy and favor the appearance of the COO [5]. It is also noted that certain typical features of the COO state depend evidently on the layered structural properties and local structural distortions, as discussed in the following sections.

$La_{0.5}Ca_{0.5}MnO_3$ has an insulating ground state with an energy gap of about 0.25 eV, as obtained by the GGA + U method for the CE-type AFM structure. The energy difference between the FM and CE-type AFM state is relatively small

Table 1. Mn-3d orbital occupancy of the majority spin and magnetic moment μ as obtained by GGA + U calculations, and the corresponding Mn formal oxidation states in several mixed-valence manganites for the AFM states. n_1 is the number of 3d electrons of the majority spin obtained by integrating over the muffin-tin radius.

	Mn-3d majority-spin occupancy					n_1	μ (μ_B)	Mn formal oxid. state
$La_{0.5}Ca_{0.5}MnO_3$	0.839	0.908	0.885	0.756	0.572	3.960	3.52	+3
	0.807	0.908	0.887	0.546	0.587	3.736	3.13	+4
$La_{0.5}Sr_{1.5}MnO_4$	0.919	0.913	0.913	0.539	0.634	3.919	3.46	+3
	0.827	0.917	0.917	0.623	0.548	3.832	3.34	+4
$LaSr_2Mn_2O_7$	0.919	0.914	0.919	0.506	0.670	3.925	3.41	+3
	0.826	0.922	0.918	0.580	0.573	3.818	3.22	+4

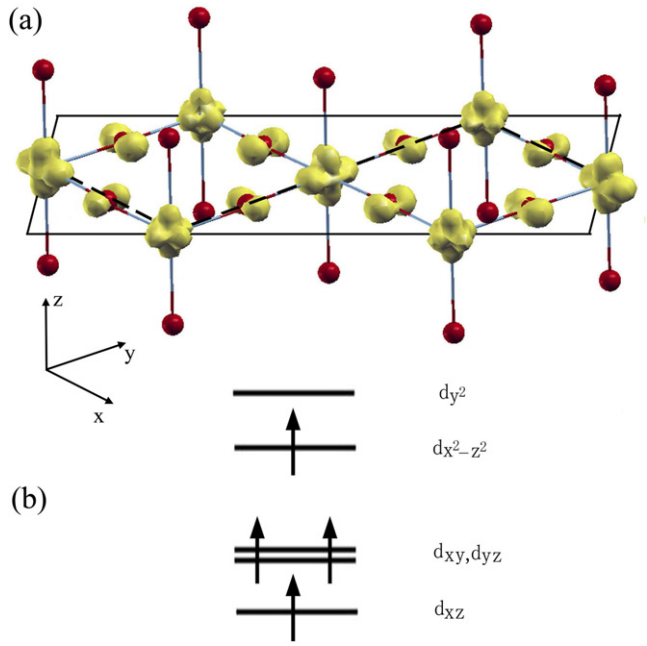

Figure 4. (a) Three-dimensional charge density contours corresponding to the e_g valence bands of $La_{0.5}Sr_{1.5}MnO_4$ (figure 2). Filled circles (red) represent O ions. (b) The schematic energy level diagrams for the majority-spin $Mn1^{3+}$-3d orbitals. The local coordinates are shown in (a), and x and y are interchangeable. The rectangle denotes the unit cell in the ab plane, and the dashed lines indicate the zigzag chains.

(21 meV per formula unit), so the coexistence of the FM metallic state and the AFM insulating state is often observed experimentally [3]. Low-temperature structural analysis [20] revealed that the Mn_2^{4+} octahedron retains a high symmetry without notable distortion. In contrast, the $Mn1^{3+}$ octahedron shows remarkable distortion, in which the Mn–O length is elongated along the $x(y)$ direction, leading to four short bonds of 1.92 Å and two long bonds of 2.06 Å along the zigzag chain, as listed in table 2. This structural distortion results in the e_g orbitals splitting into the high-lying $d_{y^2-z^2}$ ($d_{x^2-z^2}$) orbitals and low-lying d_{x^2} (d_{y^2}) orbitals. Therefore, for the Mn^{3+} sites, the low-lying d_{x^2} (d_{y^2}) orbitals would be preferentially occupied, resulting in a specific COO with zigzag chains. These data agree well with the results reported in previous literature using different theoretical methods [5, 14, 25].

Figure 2(a) shows the band structure of $La_{0.5}Sr_{1.5}MnO_4$ calculated by the GGA + U method. An insulating state with an energy gap of 0.7 eV is obtained for the CE-type AFM state. The Mn-e_g orbitals are located between about 0.60 eV below and 2.80 eV above the E_F. The charge difference of the majority spin between $Mn1^{3+}$ and $Mn2^{4+}$ ions is 0.09e which is much smaller than that in $La_{0.5}Ca_{0.5}MnO_3$ (0.22e). The notable difference between these two distinct Mn sites is the orbital occupancy as shown in the projected density of states in figures 3(a) and (b). At room temperature, the MnO_6 octahedron in the tetragonal $La_{0.5}Sr_{1.5}MnO_4$ has been actually elongated along the z direction (two long bonds of 2.07 Å along the z direction and four short bonds of 1.93 Å in the ab plane). The twofold degenerate e_g orbitals are therefore split into the high-lying $d_{x^2-y^2}$ and low-lying d_{z^2} orbitals, and the 3d electrons would prefer to occupy the low-lying d_{z^2} orbitals. Following the COO phase transition, the Mn_2^{4+} octahedron remains undistorted at low temperature. However, for the $Mn1^{3+}$ octahedron, two in-plane Mn–O bonds (1.86 Å) get contracted along the $x(y)$ direction in the COO state, while the other two in-plane Mn–O bonds (2.00 Å) get elongated along the $y(x)$ directions and are close to the out-of-plane Mn–O length (2.07 Å), as listed in table 2. Therefore, the e_g orbitals on $Mn1^{3+}$ sites are split into the high-lying d_{x^2} (d_{y^2}) and low-lying $d_{y^2-z^2}$ ($d_{x^2-z^2}$) orbitals, and 3d electrons would preferentially occupy the low-lying $d_{y^2-z^2}$ ($d_{x^2-z^2}$) orbitals (figure 4(b)), resulting in a COO pattern of zigzag chains, as illustrated in figure 4(a). This pattern is in contrast with the previously proposed one which is composed of the d_{x^2} (d_{y^2}) orbitals [17].

Theoretical analysis on the double-layer $LaSr_2Mn_2O_7$ compound reveals a relatively small energy gap (0.06 eV) and large bandwidth in comparison with the two other COO phases mentioned above, as shown in figure 2(b). The charge difference of the majority spin between $Mn1^{3+}$ and $Mn2^{4+}$ ions is about 0.11e which is slightly larger than that of $La_{0.5}Sr_{1.5}MnO_4$. For the high-symmetry structure of $LaSr_2Mn_2O_7$, the Mn atom deviates from the center of the MnO_6 octahedron, leading to two different Mn–O_{ap} bonds (2.148 and 1.848 Å, where O_{ap} denotes the apical oxygen atom) along the c-axis. In the low-temperature COO phase, the long Mn–O_{ap} bond becomes shorter (1.944 Å) and, on the contrary, the short one gets elongated to 1.922 Å, as listed in table 2. These changes as well as four contracted Mn–O bonds in ab plane lead to an increase in the bandwidth, and the twofold degenerate e_g orbitals of $Mn1^{3+}$ ions are divided into the high-lying d_{y^2} (d_{x^2}) and low-lying $d_{x^2-z^2}$ ($d_{y^2-z^2}$) orbitals with relatively small splitting, as shown in figures 3(c)

Table 2. The Mn–O distances in the $Mn1^{3+}$–$Mn2^{4+}$ charge ordered state for three mixed-valence manganites. For $LaSr_2Mn_2O_7$, there are two different Mn–O_c distances in the distorted octahedra.

	Mn1–O_a	Mn1–O_b	Mn1–O_c	Mn2–O_a	Mn2–O_b	Mn2–O_c	
$La_{0.5}Ca_{0.5}MnO_3$	2.056	1.920	1.915	1.917	1.915	1.915	[20]
$La_{0.5}Sr_{1.5}MnO_4$	2.003	1.859	2.070	1.930	1.930	2.070	[21]
$LaSr_2Mn_2O_7$	1.919	1.842	1.921 1.944	1.874	1.824	1.922 1.944	[22]

and (d). As a result, the majority of electrons would prefer to occupy the low-lying $d_{x^2-z^2}$ ($d_{y^2-z^2}$) orbitals, and the COO pattern would be similar to that in $La_{0.5}Sr_{1.5}MnO_4$. So, it would be more suitable to consider the magnetic structure as the CE-type AFM [26] rather than the A-type one. It is also noted that the relatively large bandwidth and the small energy splitting of the e_g orbitals would effectively reduce the difference of orbital occupancy between the $d_{x^2-z^2}$ ($d_{y^2-z^2}$) and d_{y^2} (d_{x^2}) orbitals, as illustrated in the orbitally projected density of states (figures 3(c) and (d)) which show a relatively small difference between two distinct Mn sites compared with single-layer $La_{0.5}Sr_{1.5}MnO_4$, so that the CE-type AFM state would be unstable and easily replaced by other ordered states. As observed in experiments, the COO occurring at $T_{CO} = 225$ K starts melting following the AFM transition ($T_N = 170$ K), as demonstrated by the measurement of structural and physical properties [23], and complex reentrance phase transitions, in correlation with the e_g-orbital ordering, appear in $La_{2-2x}Sr_{1-x}Mn_2O_7$ at low temperature [10, 26].

Note that the difference of the majority-spin 3d electrons (n_1) between two distinct Mn sites (0.1–0.2e) is different among these three compounds and is actually far less than the nominal ionicity difference of $+1e$, as listed in table 1. In addition, this difference of charge is also less than that of the magnetic moment (spin value), as illustrated in figure 5. This difference between charge and spin values could be considered to originate from the strong hybridization between Mn-3d and O-2p states with the subsequent screening of Mn charge by electrons in surrounding O atoms [5]. Therefore, it is evident that the chemical bonding with respect to the layered structures and local distortions results in different charge differences in these compounds, which coincides with the argument that the origin of the charge ordering is due to the JT distortions [14].

As far as the on-site Coulomb interaction (U) is concerned, it is thought that the charge ordering is enhanced by the electronic correlation and that the magnitude of the charge difference monotonously increases with U. On the other hand, the inclusion of strong local correlations is argued to impair the agreement with the experimental data [27]. We calculated the U dependence of the charge difference between two distinct Mn sites for $La_{0.5}Ca_{0.5}MnO_3$, as shown in figure 5, and it is noted that the charge disproportionation still exists in the absence of the electron correlation, in agreement with the previous calculations [14]. In addition, our calculations show that the difference of the charge (Δn_e) as well as the difference of the magnetic moment (Δn_m) exhibits a maximum at $U \approx 5$ eV, although the magnetic moments as well as the total charge of two Mn sites monotonously increase with U due to the increased localization. This result indicates that the strong

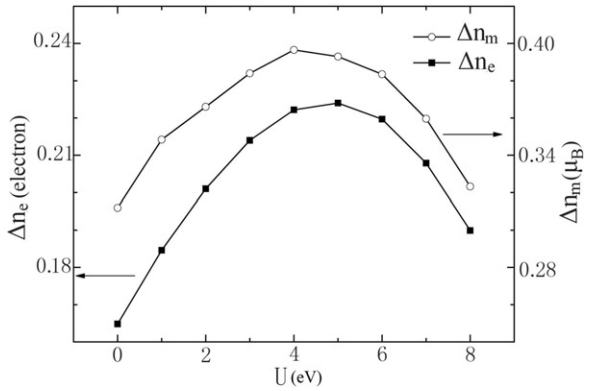

Figure 5. On-site Coulomb interaction (U) dependence of the differences of charge (Δn_e) and magnetic moment (Δn_m) between two distinct Mn sites for $La_{0.5}Ca_{0.5}MnO_3$.

electron correlation is not essential for the COO and that the inclusion of the proper magnitude of the electron correlation is important to get better agreement with the experimental data.

As discussed above, these three typical compounds have different layered structures and dissimilar structural modifications in association with the COO transition at low temperature. All three COO patterns consist of similar zigzag chains in the ab plane despite the orbital occupancy being very different. From a structural point of view, these three COO patterns would give rise to superstructures with an identical periodicity, as demonstrated by x-ray measurements and TEM observations [9–11]. However, their physical properties, especially the electronic states and orbital occupancy, are very different from one another. That is, the orbital ordering and the orbitally driven phase transitions are sensitive to their specific layered structural features which give rise to different bandwidths and dimensionalities.

In summary, the COO in mixed-valence manganites $La_{1.5}Sr_{0.5}MnO_4$ ($n = 1$), $LaSr_2Mn_2O_7$ ($n = 2$), and $La_{0.5}Ca_{0.5}MnO_3$ ($n = \infty$) have been investigated by first-principles calculations. The theoretical results suggest that the low-temperature COO patterns and orbital occupancy are closely related to the layered structural features. The single-layer $La_{0.5}Sr_{1.5}MnO_4$ as well as the double-layer $LaSr_2Mn_2O_7$ exhibits zigzag-chain orbital ordering composed of the $d_{y^2-z^2}$ ($d_{x^2-z^2}$) orbitals in contrast with the d_{z^2} orbitals in $La_{0.5}Ca_{0.5}MnO_3$. Systematical analysis revealed that the dominant factor responsible for the COO in these compounds is the structural distortions, and one must also consider the contributions from the on-site Coulomb interaction and magnetic interaction in order to obtain the correct ground state.

Acknowledgments

The work reported here is supported by the National Science Foundation of China, Chinese Academy of Sciences and the Ministry of Science and Technology of China.

References

[1] Dagotto E, Hotta T and Moreo A 2001 *Phys. Rep.* **344** 1
[2] Moreo A, Yunoki S and Dagotto E 1999 *Science* **283** 2034
[3] Loudon J C, Mathur N D and Midgley P A 2002 *Nature* **420** 797
[4] Mori S, Chen C H and Cheong S-W 1998 *Nature* **392** 473
[5] Ferrari V, Towler M and Littlewood P B 2003 *Phys. Rev. Lett.* **91** 227202
[6] Imada M, Fujimori A and Tokura Y 1998 *Rev. Mod. Phys.* **70** 1039
[7] Goodenough J B 1955 *Phy. Rev.* **100** 564
[8] Tokura Y and Nagaosa N 2000 *Science* **288** 462
[9] Li J Q, Uehara M, Tsuruta C, Matsui Y and Zhao Z X 1999 *Phys. Rev. Lett.* **82** 2386
[10] Li J Q, Matsui Y, Kimura T and Tokura Y 1998 *Phys. Rev.* B **57** R3205
[11] Wilkins S B, Spencer P D, Hatton P D, Collins S P, Roper M D, Prabhakaran D and Boothroyd A T 2003 *Phys. Rev. Lett.* **91** 167205
Murakami Y, Kawada H, Kawata H, Tanaka M, Arima T, Moritomo Y and Tokura Y 1998 *Phys. Rev. Lett.* **80** 1932
[12] Huang D J, Wu W B, Guo G Y, Lin H-J, Hou T Y, Chang C F, Chen C T, Fujimori A, Kimura T, Huang H B, Tanaka A and Jo T 2004 *Phys. Rev. Lett.* **92** 087202
[13] Mutou T and Kontani H 1999 *Phys. Rev. Lett.* **83** 3685
[14] Popovic Z and Satpathy S 2002 *Phys. Rev. Lett.* **88** 197201
[15] Attfield J P, Bell A M T, Rodriguez-Martinez L M, Greneche J M, Cernik R J, Clarke J F and Perkins D A 1998 *Nature* **396** 655
[16] Leonov I, Yaresko A N, Antonov V N, Attfield J P and Anisimov V I 2005 *Phys. Rev.* B **72** 014407
[17] Mahadevan P, Terakura K and Sarma D D 2001 *Phys. Rev. Lett.* **87** 066404
[18] Herrero-Martín J, García J, Subías G, Blasco J and Concepción Sánchez M 2004 *Phys. Rev.* B **70** 024408
[19] Blaha P, Schwarz K, Madsen G, Kvasnicka D and Luitz J 2001 *WIEN2K, An Augmented Plane Wave + Local Orbital Program for Calculating Crystal Properties* Karlheinz Schwarz, Technical University, Wien, Austria
[20] Radaelli P G, Cox D E, Marezio M and Cheong S-W 1997 *Phys. Rev.* B **55** 3015
[21] Zeng L J, Ma C, Yang H X, Xiao R J, Li J Q and Jansen J 2008 *Phys. Rev.* B **77** 024107
[22] Argyriou D N, Bordallo H N, Campbell B J, Cheetham A K, Cox D E, Gardner J S, Hanif K, dos Santos A and Strouse G F 2000 *Phys. Rev.* B **61** 15269
[23] Chatterji T, McIntyre G J, Caliebe W, Suryanarayanan R, Dhalenne G and Revcolevschi A 2000 *Phys. Rev.* B **61** 570
[24] Fang Z and Nagaosa N 2004 *Phys. Rev. Lett.* **93** 176404
[25] Tyer R, Temmerman W M, Szotek Z, Banach G, Svane A, Petit L and Gehring G A 2004 *Europhys. Lett.* **65** 519
[26] Li Q A, Gray K E, Zheng H, Claus H, Rosenkranz S, Ancona S N, Osborn R, Mitchell J F, Chen Y and Lynn J W 2007 *Phys. Rev. Lett.* **98** 167201
[27] Luo W, Franceschetti A, Varela M, Tao J, Pennycook S J and Pantelides S T 2007 *Phys. Rev. Lett.* **99** 036402